Talanta 233 (2021) 122592

Contents lists available at ScienceDirect

Talanta

journal homepage: www.elsevier.com/locate/talanta

A novel water-soluble near-infrared fluorescent probe for monitoring mitochondrial viscosity

Siqi Zhang [a], Yu Zhang [b], Lihe Zhao [a], Lanlan Xu [a], Hao Han [a], Yibing Huang [b], Qiang Fei [a], Ying Sun [a], Pinyi Ma [a,**], Daqian Song [a,*]

[a] College of Chemistry, Jilin Province Research Center for Engineering and Technology of Spectral Analytical Instruments, Jilin University, Qianjin Street 2699, Changchun, 130012, China

[b] College of Life Sciences, Jilin University, Qianjin Street 2699, Changchun, 130012, China

ARTICLE INFO

Keywords:
Viscosity
Mitochondria targeting
Near infrared fluorescence
Mitochondrial autophagy

ABSTRACT

Mitochondria, the main source of energy of cells, play a significant role in aerobic respiration process. Some stimulants can result in changes of mitochondrial microenvironments such as viscosity, pH and polarity. Abnormal changes of mitochondrial viscosity have been shown to relate to pathological activities and diseases. Therefore, it is critical to focus our attention on mitochondrial viscosity under different conditions. A novel organic water-soluble molecule called JLQL that could monitor viscosity was conveniently synthesized in two steps. The near-infrared sensor with maximum emission wavelength of 734.6 nm and the Stokes shift of 134.6 nm consisted of a fluorophore and a mitochondrial-targeting moiety as an acceptor group; the two were connected by a double bond. The fluorescence intensity of the sensor increased 175 times with the enhancement of viscosity of a PBS-glycerol system. The interference of other microenvironments such as pH and polarity and other interference analytes could be reduced. JLQL could sensitively and selectively differentiate different levels of mitochondrial viscosity induced by monensin or nystatin. Furthermore, the probe may provide an attractive way to monitor real-time changes of viscosity during mitophagy. Possessing the above properties, JLQL can potentially be employed as a powerful tool for the observation of mitochondrial viscosity.

1. Introduction

Viscosity, which serves as one of the most important intracellular environments, is an essential factor affecting the transmission of mass and signals, as well as the protein-protein interactions in cellular membranes [1–5]. Variation of intracellular viscosity has been demonstrated to be an indicator for cell malignancy [6], diabetes [3,7], atherosclerosis [8], Alzheimer's disease [9] and so on. The viscosity of different organelles varies greatly even in the same type of cells [10–12]. To better investigate the effects of viscosity changes in cells, it is probably of greater significance to perform the detection in specific organelles rather than in the whole cytoplasm [10].

As one of the most abundant organelles in cells, mitochondria could be a key site for aerobic respiration to provide energy for various activities of cells [13,14]. Some neurodegenerative diseases such as Parkinson's and Huntington's disease are found to be related to the disruption of mitochondrial dynamics [15,16]. Mitochondrial viscosity is closely related to cellular respiration, as it can affect cellular metabolite diffusion and apoptosis, and can regulate mitochondrial metabolism [4]. Therefore, it is urgent to engineer a molecular probe that is suitable for visualizing mitochondrial viscosity. The traditional viscosity measurement methods can only measure the viscosity of macroscopic liquid, while are also time-consuming and unable to measure the viscosity of organelles [17,18]. To solve these problems, small molecular fluorescent probes, which have attracted broad attention, have been developed for visualization of biological microenvironments including pH [19,20], amino acid [21,22], viscosity [23,24] and polarity [25] by transforming recognition information into fluorescent signals. Near-infrared emission could minimize the interference by cell autofluorescence and the photodamage to living cells and organisms [24]. A large Stokes shift has some inherent advantages such as low background fluorescence, noninvasiveness and high sensitivity [26]. Up to now, fluorescence confocal imaging is regarded as one of the most important methods for monitoring biological processes due to its advantages such

* Corresponding author.
** Corresponding author.
E-mail addresses: mapinyi@jlu.edu.cn (P. Ma), songdq@jlu.edu.cn (D. Song).

https://doi.org/10.1016/j.talanta.2021.122592
Received 16 March 2021; Received in revised form 31 May 2021; Accepted 5 June 2021
Available online 8 June 2021

as real-time visualization ability and rapid response [27,28].

In this article, a novel near-infrared fluorescent probe was designed and synthesized for use in visualization of viscosity changes. Modified julolidine group was chosen as the fluorophore to increase the emission wavelength to as close to the near-infrared wavelength as possible, and quinoline derivative cation was used to target mitochondria. The two groups were linked through a double bond to form a rotating site. Owing to its large Stokes shift, JLQL had low background interference, and its signals were non-destructible, thus could be used as a selective and sensitive probe for tracking changes of intracellular viscosity. Variation of fluorescence signals was based on the twisted intramolecular charge transfer (TICT) principle, which was the competition between the radiation attenuation of the excited electrons in the fluorophore and the intramolecular conversion [29]. JLQL with quinoline derivative cation was soluble in water; it could enter into the cells and had low cytotoxicity. The stimulation by ionic carriers could induce the swelling of mitochondrial ultrastructure or other changes, leading to the increase of viscosity [27,30]. Toward this end, JLQL could accurately monitor different levels of mitochondrial viscosity during this process. JLQL could monitor the overall viscosity changes during mitochondrial autophagy. Collectively, JLQL with near-infrared emission and large Stokes shift has a sound prospect and it can be applied to study various physiological processes. Fortunately, the sensor JLQL could also promisingly be used as a platform for mapping viscosity in the mitochondrial matrix and as a tool in fundamental research.

2. Materials and procedures

2.1. Materials and instruments

The materials and instruments used in the work could be found in the supplementary information.

2.2. Synthesis of probe JLQL

The synthetic route of JLQL is shown in Fig. 1.

2.2.1. Compound 2

The material for the synthesis of compound 2 was 4-methyl quinoline and iodomethane so that it was iodide. Compound 2 was synthesized based on the previously reported literature [31,32].

2.2.2. JLQL

The reaction condition between compound 1 and 2 referred to the synthetic procedure of a similar molecule reported in the previous literature [33]. 8-hydroxyjulolidine-9-carboxaldehyde (137.22 mg, 0.632 mmol) and compound 2 (100 mg, 0.632 mmol) were dissolved in 35 mL of ethanol in a dry flask. After piperidine (248.7 μL) was added to the mixture, the reaction was refluxed and stirred at 80 °C for 12 h. The product was purified by TLC using a solution consisting of dichloromethane and methanol (35:1) as the eluent. JLQL, a deep blue solid, was obtained and collected (47 mg, 21%). ^{1}H NMR (400 MHz, $CDCl_3$) δ 8.67 (d, 1H), 8.46 (t, 2H), 8.27 (d, 1H), 8.09 (dd, 1H), 7.93–7.85 (m, 1H), 7.80 (d, 1H), 7.68 (t, 1H), 7.43 (d, 1H), 4.27 (s, 3H), 3.33 (ddd, 5H), 2.80–2.72 (m, 3H), 2.11–1.86 (m, 5H). MS (ESI): Calcd for $[C_{24}H_{25}N_2O]^+$: 357.20, found: 357.16.

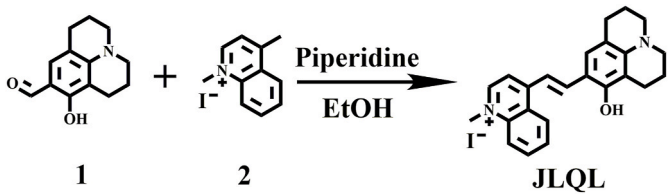

Fig. 1. Synthetic route of JLQL.

2.3. Sample treatment and spectrophotometry

2.3.1. Sample treatment

JLQL was dissolved in ultrapure water to prepare a stock solution at a concentration of 1 mM; the solution was stored at −40 °C and in the dark. Glycerol at different ratios was thoroughly mixed with PBS (pH = 7.40, 10 mM) and was used to change the viscosity of the solvent. Viscosity was prepared by a corrected NDJ-5S digital rotational viscometer and the values could be read directly. The stock solution of the probe (20 μL) was added to the solvents (980 μL) with different viscosities, and the solutions were subjected to ultrasound treatment in an ultrasonic cleaner at a constant temperature of 37 °C to eliminate air bubbles. The final concentration of the probe was 20 μM. UV–Vis absorption and fluorescence spectra were remained at the same condition. It is worth mentioning that $\log I_{734.6}$ of JLQL had a linear relationship with $\log\eta$ (viscosity), which could be described by the Forster–Hoffmann equation:

$$\log(I) = C + x \log \eta$$

where I is the emission fluorescence intensity; η is the solvent viscosity; c is a constant; and x is the dye-dependent constant.

2.3.2. Response of the probe to pH and polarity

The stock solution of JLQL (20 μL) was added to a mixture containing 980 μL PBS (pH = 7.40, 10 mM) at different pH values and glycerol at the same proportion to prepare solutions with different pH values (1.15, 2.17, 4.97, 6.02, 7.43, 7.90, 9.07, 10.67, 11.27, 11.96, 12.90, and 13.12). JLQL (20 μL) was added into DMF, DMSO, EtOH, or CH_3CN (each at 980 μL) to prepare probe solutions with different polarities. The final concentration of the probe was 20 μM as well. All the trials were conducted at a constant temperature of 37 °C.

2.3.3. Response of the probe to different interference analytes

To investigate the selectivity of the probe, interfering species, including Zn^{2+}, Na^+, Mn^{2+}, Li^+, Ca^{2+}, Ag^+, Cu^{2+}, HPO_4^{2-}, CN^-, Cl^-, Cys and GSH were added to PBS (pH = 7.40, 10 mM) to prepare solutions containing different analytes. The final concentration of the analytes was 50 μM, and the final concentration of the probe was 20 μM.

2.3.4. Measurement of optical stability of probe

To verify the photostability of the probe under laser irradiation to ensure the feasibility in subsequent experiments, the probe was subjected to continuous irradiation by laser light for 60 min in low and high viscosity conditions, and the fluorescence intensity was measured every 2 min.

2.4. Cell imaging experiments

2.4.1. Co-staining experiment

The co-localization experiment was carried out using commercial dyes: MitoTracker Green and LysoTracker. A549 cells were co-incubated with the probe JLQL (20 μM) and MitoTracker Green (20 nM) for 35 min. To further explore the co-localization ability of the probe with other organelles such as lysosomes, A549 cells were co-incubated with the probe JLQL (15 μM) and LysoTracker (20 nM) for 35 min. The A549 cells were washed three times with PBS and then subjected to imaging.

2.4.2. Fluorescence imaging of viscosity in A549 cells

Monitoring of cellular viscosity changes induced by monensin or nystatin: A549 cells were incubated with monensin or nystatin (each at a final concentration of 6 μM) for 20 min, followed by the probe JLQL (15 μM) for 30 min.

Monitoring of cellular viscosity changes induced by serum-free medium: A549 cells were incubated with JLQL (15 μM) in serum-free medium for 0.5 h or 2 h.

The cells were washed three times with PBS before being subjected to imaging. And the imaging was carried out by a fluorescence confocal microscope.

3. Results and discussion

3.1. Spectral response of the probe JLQL

First, we designed the molecule that could be easily synthesized and it was suitable for non-toxic biological applications. In order to make the molecule become more sensitive to rotation so that it can better realize TICT principle, we added a double bond between the NIR fluorophore (the modified julolidine group) and quinoline derivative cation of JLQL to form a rotation site, and the introduction of quinoline derivative cation expanded the conjugated structure of the molecule to increase its maximum emission wavelength to near-infrared region (734.6 nm). We designed the molecule to contain quinoline derivative cation so that it could target the mitochondria. Fortunately, the probe was highly soluble in water due to the cationic form of JLQL; thus, it had good biocompatibility. What's more, we explored the fluorescence response to viscosity of JLQL. Spectral response to viscosity of the probe JLQL was recorded in the solvents containing glycerol at different gradient ratios. The UV–Vis absorption peak at 610 nm increased with the increase of solvent viscosity (from 0.96 to 379.5 cP) (Figure S1). The fluorescence emission peak at 734.6 nm in Fig. 2A greatly enhanced as glycerol was gradually added, and the fluorescence intensity at the highest viscosity was about 175 times more than that at the lowest viscosity. In a low viscosity solvent, the rotor could rotate freely so that the fluorescence emission was somewhat inhibited. By contrast, in a high viscosity solvent, the rotor rotation was limited, and the energy could only be released in the form of fluorescence [34,35]. The mechanism explained why JLQL was highly sensitive to viscosity. The large Stokes shift of 134.6 nm could avoid the interference from the autofluorescence. Values within the range of mitochondrial viscosity were analysed for the linear relationship to better study viscosity variation in mitochondria. As shown in Fig. 2B, a log–log plot of intensity I versus solvent viscosity (η) ranging from 0.96 to 105.7 cP, the probe JLQL had a linear relationship ($R^2 = 0.9955$) that conformed to the Förster–Hoffmann equation. The quantum yield of the probe JLQL was 0.77% in PBS and was 3.28% in 99% glycerol. The rotation process of the rotor was inhibited by high-viscosity environment, reducing probability of non-radiative transition, and thus resulting in the increase of fluorescence intensity and quantum yield.

JLQL had excellent optical stability in both low- and high-viscosity environments (Figure S2), indicating that the probe was not readily decomposed under light. To demonstrate the specificity of JLQL to viscosity, we conducted the experiment at various pH values. The probe was added to a series of solvents containing PBS and glycerol at the same proportion but different pH values, and the final concentration of the probe was 20 μM. The probe JLQL was kept at 37 °C to ensure that the experimental conditions were consistent. The fluorescence intensity was measured at an excitation wavelength of 600 nm. The fluorescence intensity of the probe JLQL was relatively stable at various pH values, indicating that it was not sensitive to pH compared with viscosity (Figure S3). To investigate the response of the probe JLQL to polarity and other interference analytes commonly found in cells, we conducted polarity experiment, and interference experiment in the presence of different cations, anions, and amino acids including Zn^{2+}, Na^{+}, Mn^{2+}, Li^{+}, Ca^{2+}, Ag^{+}, Cu^{2+}, HPO_4^{2-}, CN^{-}, Cl^{-}, Cys and GSH in PBS, which were mixed with the probe prior to recording their fluorescence spectra. Compared with that of glycerol, the effect of polarity and the above interfering substances on JLQL was negligible (Figures S4-S5). This

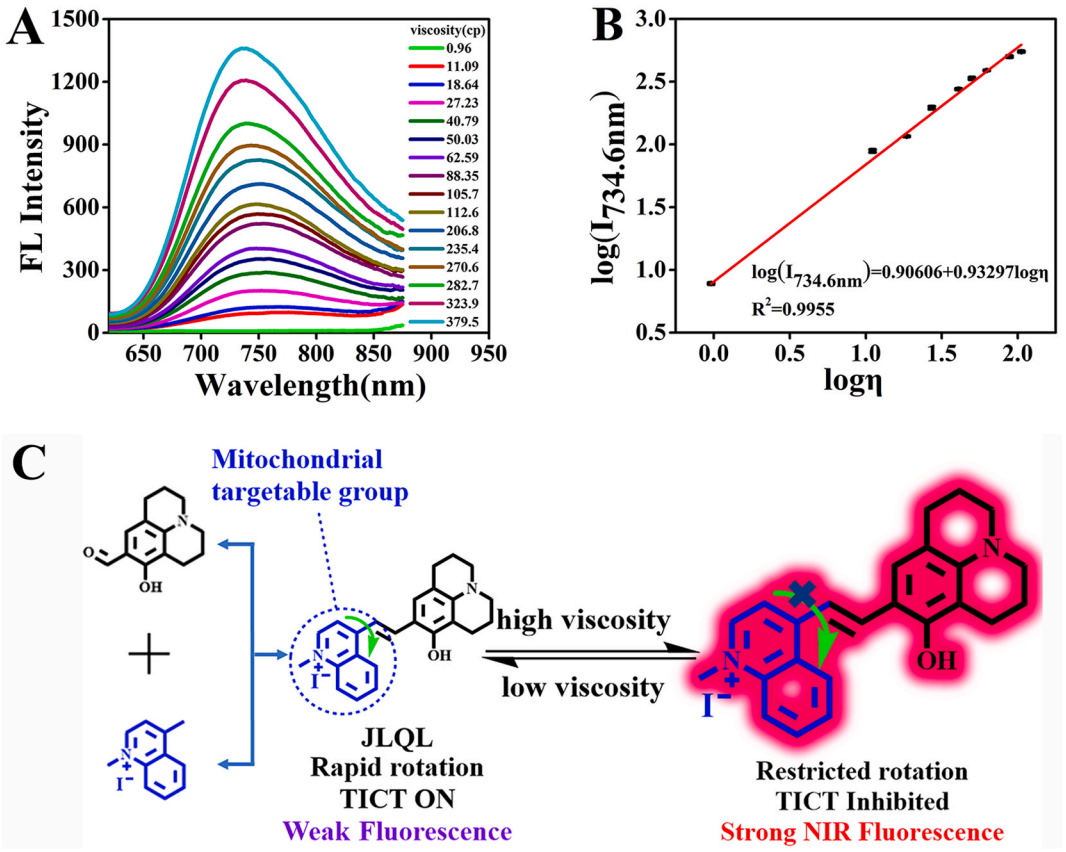

Fig. 2. (A) Fluorescence spectra of JLQL in PBS–glycerol system of various glycerol ratios. (B) Linear relationship between log $I_{734.6}$ and log η of the probe JLQL, λex = 600 nm. (C) Designed structure and response mechanism to viscosity of JLQL.

illustrated that JLQL could not be affected by factors other than the microenvironmental viscosity changes.

3.2. Theoretical calculations

To further shed light on the observed relationship between fluorescence enhancement and viscosity and provide a reasonable explanation to it, theoretical calculations were performed, and the result was shown in Fig. 3. At the ground state (S_0), the dihedral angles θ_1 and θ_2 were 0.33° and 0.76°, respectively, and the structure of JLQL was nearly planar. The HOMO and LUMO were located in the whole molecule and had local excitation (LE) properties. The fluorophore in the LE state had a quasi-planar molecular conformation and was highly fluorescent. For the S_1 state, the fluorophore could undergo a transition from the initially LE state to the TICT state. For the JLQL in its ~90°-twisted excited state, the HOMO was located on the julolidine group, while the LUMO was located in the quinoline group; this resulted in the apparent charge separation. Consequently, the TICT states of the rotors could inhibit the fluorescence emission of JLQL, causing it to become nearly non-fluorescent. To explain whether the TICT process of JLQL is generable, the changes in the potential energy of the S_0 and S_1 states of JLQL as a function of the dihedral angle θ_1 were calculated. Previous studies have shown that the rotation barrier (E_{RB}) and the driving energy (E_{DE}) are crucial parameters for evaluating the transition from the LE state to the TICT state. When the E_{RB} does not exist and the $E_{DE} < 0$ (−1.04 eV), the occurrence of TICT states is spontaneous. This result shows that the enhancement of fluorescence intensities of JLQL in glycerol is due to TICT inhibition because glycerol is significantly more viscous than water, thus causing the rotation of the molecule to be impeded.

3.3. Detection of viscosity in PBS and lactulose oral solution system

We also explored the application of JLQL in actual sample (lactulose oral solution). PBS and lactulose oral solution were mixed in different proportions to prepare solutions with different viscosity values, and then JLQL (20 μL) was added to record the fluorescence intensity of the actual sample under the same conditions. The viscosity values measured by the method of fluorescence spectra were obtained according to the linear relationship mentioned above. The results showed that the difference between the measured viscosity and the standard viscosity (values measured by the viscometer) was small and showed good precision (Table 1). We also calculated the confidence limit ($t = 2.68 < t_{0.01,9}$) when the ratio of lactulose oral solution in PBS and lactulose oral solution system was 77%, and the result proved no significant difference, which proved the feasibility of the method.

Table 1
Analytical results of PBS and lactulose oral solution system (n = 5).

Sample No.	Standard values (cP)	Found (cP)	RSD (%)
1	9.94	10.8	1.92
2	24.7	23.9	3.68
3	54.1	47.9	4.93

3.4. Cytotoxicity and imaging of cell co-localization

MTT assay was employed to investigate the toxicity of JLQL to A549 cells. The calculation results showed that the cell survival was highest in the presence of JLQL at a concentration of 10 μM, implying that 10 μM JLQL had the lowest cytotoxicity (Figure S6). However, due to the low concentration (10 μM) of JLQL, the resolution of the image was too low, and the cells could not be observed clearly. Therefore, we used higher concentrations as the optimal conditions in the cell experiments.

To explore the localization of JLQL in different organelles, we conducted co-localization experiments by using A549 cells. Based on the above discussion, 20 μM JLQL and mitochondrial dye MitoTracker Green were co-incubated for 35 min before being subjected to cell imaging by confocal microscopy. According to the results depicted in Fig. 4F, the red channel of JLQL overlapped with the green channel of MitoTracker Green, and the Pearson's correlation coefficient reached almost 0.95. The Pearson's correlation coefficient for the co-localization of JLQL and lysosome was only 0.22, showing that there was almost no overlap between JLQL and lysosome (Figure S7). These results indicate that JLQL is localized in mitochondria, thus could be widely used as a mitochondria-targeted probe in biological systems. In addition, as a small organic molecule, JLQL could rapidly enter into A549 cells through osmosis, which further demonstrates its biocompatibility and promising biological applications.

3.5. Detection of changes of intracellular viscosity

As shown in Fig. 5A1-5B1, the fluorescence of JLQL was relatively obvious to that of the control cells, due to its unique chemical structure. Monensin is a polyether antibiotic and an ion carrier that can carry cations across the cell membrane, which in turn causes the changes of concentration of intracellular ions. Through this process, a large amount of water can enter into the cells, causing them to swell and deform, in turn leading to cell apoptosis. During this process, monensin causes changes of viscosity in mitochondria [36]. To prove that JLQL can be used to observe the changes of mitochondrial viscosity caused by monensin, monensin was added into A549 cells to induce changes of cell microenvironment, and JLQL was then added to monitor the changes.

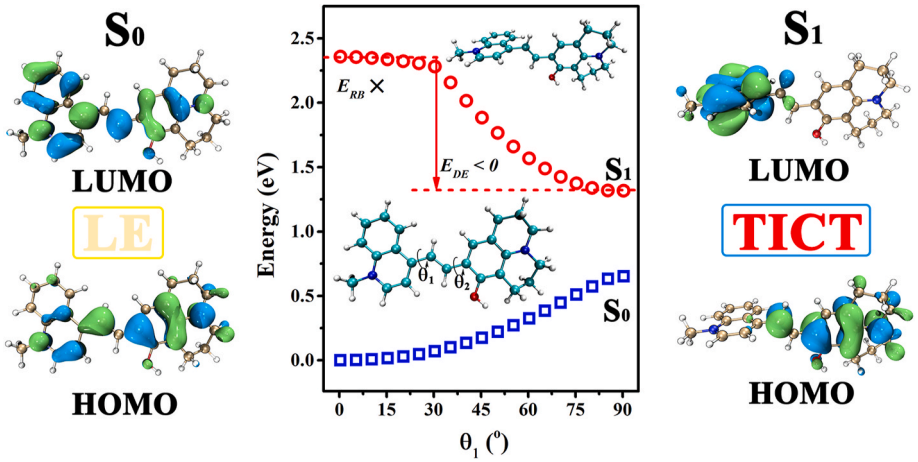

Fig. 3. Theoretical models illustrating the HOMO/LUMO energy level and the relevant frontier molecular orbitals of JLQL. The TDDFT calculations of the LE→TICT photoreaction represented by a plot of S_0 and S_1 energy versus rotation angle (θ_1) as the formation of LE/TICT excited states progressed.

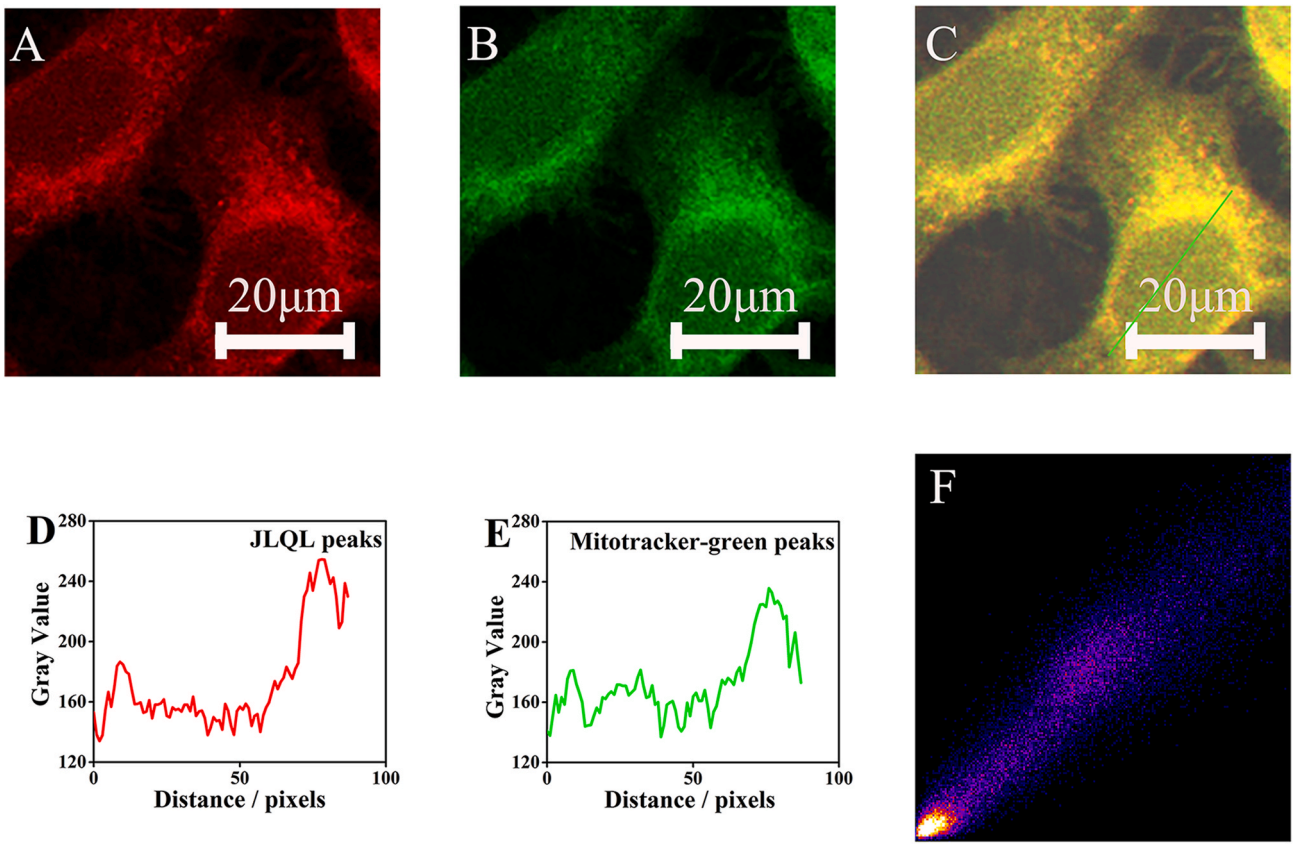

Fig. 4. Co-localization studies of JLQL in mitochondria. (A) Red channel of JLQL (λex = 633 nm, λem = 640–750 nm). (B) Green channel of Mito-tracker Green (λex = 490 nm, λem = 415–635 nm). (C) Overlay of (A) and (B). (D) Signal profile of the red channel. (E) Signal profile of the green channel. (F) The Pearson's correlation coefficient for the overlap between JLQL and Mito-Tracker green, which was 0.95. (For interpretation of the references to colour in this figure legend, the reader is referred to the Web version of this article.)

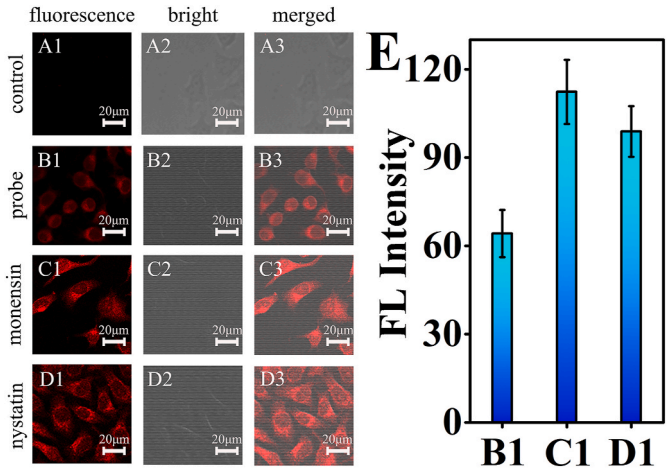

Fig. 5. Fluorescence images of A549 cells incubated with monensin and nystatin. Fluorescence (A1) and bright-field (A2) images of control cells, and their merged image (A3). Fluorescence (B1) and bright-field (B2) images of A549 cells incubated with only 15 μM JLQL, and their merged image (B3). Fluorescence (C1) and bright-field (C2) images of A549 cells incubated with 6 μM monensin for 20 min, followed by 15 μM JLQL for another 30 min, and their merged image (C3). Fluorescence (D1) and bright-field (D2) of A549 cells incubated with 6 μM nystatin for 20 min, followed by 15 μM JLQL for another 30 min, and their merged image (D3). (E) Fluorescence intensity of images in (B1), (C1) and (D1).

After that, the fluorescence intensity of JLQL were observed both under a fluorescence confocal microscope. As shown in Fig. 5C1-5C3 and 5 E, we found that the fluorescence intensity of cells pretreated with monensin was enhanced, indicating that the cellular viscosity was increased. The results also showed that monensin could induce the microenvironmental change of mitochondria by increasing their viscosity.

Nystatin is a polyene antibiotic that can cause changes of cell structures and swelling of mitochondria that leads to a series of mitochondrial diseases [36]. Nystatin, like monensin, could also cause variation of mitochondrial viscosity. Similarly, A549 cells were incubated with nystatin, followed by JLQL, and were then observed under bright and fluorescence fields. A549 cells with nystatin exhibited stronger fluorescence intensity compared to those without nystatin, as illustrated in Fig. 5D1-5D3 and 5 E. This indicated that nystatin could cause mitochondrial swelling, which was consistent with the results previously reported in the literature.

Mitochondrial autophagy is a form of self-regulation. In the absence of external nutrition or other stimulations, mitochondria can be depolarized and damaged, and in order to maintain cellular balance and stability, the damaged mitochondria are then fused with and degraded in lysosomes to produce energy to nourish cells [37,38]. Here, we used serum-free medium to induce mitophagy. To compare mitochondrial viscosity during mitophagy with that during the normal state, we investigated the changes of mitochondrial viscosity during mitophagy at different times by incubating A549 cells with JLQL in normal medium for 0.5 h, in serum-free medium for 0.5 h and in serum-free medium for 2 h. The fluorescence intensity of A549 cells incubated in serum-free medium was higher than that of cells incubated in normal medium, as shown in Fig. 6A1-6B3. As the mitophagy time was prolonged from 0.5 h to 2 h, the fluorescence intensity enhanced significantly, and the

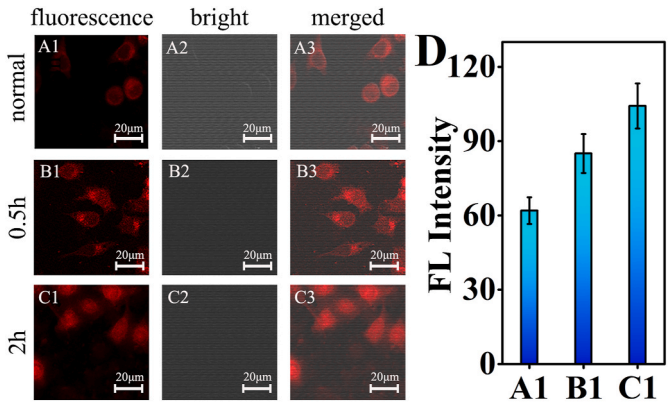

Fig. 6. Fluorescence images showing mitophagy induced by serum-free medium. Fluorescence (A1) and bright-field (A2) images of A549 cells incubated with 15 μM JLQL in normal medium for 0.5 h, and their merged image (A3). Fluorescence (B1) and bright-field (B2) images of A549 cells incubated with 15 μM JLQL in serum-free medium for 0.5 h, and their merged image (B3). Fluorescence (C1) and bright-field (C2) images of A549 cells incubated with 15 μM JLQL in serum-free medium for 2 h, and their merged image (C3). (D) Fluorescence intensity of images in (A1), (B1) and (C1).

changes of cell morphology could also be more obviously observed (Fig. 6C1-6C3), demonstrating the occurrence of mitophagy. According to the above results, it could be speculated that during the mitochondrial autophagy, mitochondrial viscosity gradually increased with increasing time. Overall, all the results demonstrated that JLQL could be used as a specific and sensitive sensor to monitor the changes of mitochondrial viscosity in many cellular applications.

4. Conclusions

In summary, we have successfully developed a novel water-soluble red-emitting fluorescent probe JLQL that could monitor the changes of viscosity in biological systems. The synthesis of JLQL was simple and could be completed in only two steps, and the reaction was also facile and convenient. JLQL had many natural advantages such as high response, low cytotoxicity, and low background interference; it also possessed eminent selectivity and specificity. Satisfactory response mechanism to viscosity of the probe was attributed to its twisted intramolecular charge-transfer ability in both low- and high-viscosity solvents. Rather than measuring viscosity in the entire cytoplasmic matrix, the developed JLQL could specially map the viscosity in mitochondria, and could monitor the increase of mitochondrial viscosity of cells treated with monensin or nystatin. Moreover, the probe was able to reflect viscosity variation during mitochondrial autophagy. These results suggest that JLQL could be used as a tool for visualization of viscosity and could be applied to rapidly identify diseases caused by changes of mitochondrial viscosity.

Credit author statement

Siqi Zhang: Conceptualization, Methodology, Visualization, Writing – original draft. Yu Zhang: Investigation, Formal analysis. Lihe Zhao: Software, Data curation. Lanlan Xu: Writing – original draft. Hao Han: Writing – original draft. Yibing Huang: Resources, Investigation. Qiang Fei: Writing – review & editing. Ying Sun: Writing – review & editing. Pinyi Ma: Supervision, Project administration, Funding acquisition. Daqian Song: Conceptualization, Supervision, Investigation, Funding acquisition.

Declaration of competing interest

The authors declare that they have no known competing financial interests or personal relationships that could have appeared to influence the work reported in this paper.

Acknowledgments

This work was supported by the National Natural Science Foundation of China (Grant nos. 22004046 and 22074052), Science and Technology Developing Foundation of Jilin Province (Grant No. 20200602047ZP).

Appendix A. Supplementary data

Supplementary data to this article can be found online at https://doi.org/10.1016/j.talanta.2021.122592.

References

[1] Z. Yang, J. Cao, Y. He, J.H. Yang, T. Kim, X. Peng, J.S. Kim, Macro-/micro-environment-sensitive chemosensing and biological imaging, Chem. Soc. Rev. 43 (13) (2014) 4563–4601.
[2] K. Luby-Phelps, The physical chemistry of cytoplasm and its influence on cell function: an update, Mol. Biol. Cell 24 (17) (2013) 2593–2596.
[3] O. Nadiv, M. Shinitzky, H. Manu, D. Hecht, C.T. Roberts Jr., D. LeRoith, Y. Zick, Elevated protein tyrosine phosphatase activity and increased membrane viscosity are associated with impaired activation of the insulin receptor kinase in old rats, Biochem. J. 298 (Pt 2) (1994) 443–450.
[4] G.J. Nie, A.D. Sheftel, S.F. Kim, P. Ponka, Overexpression of mitochondrial ferritin causes cytosolic iron depletion and changes cellular iron homeostasis, Blood 105 (5) (2005) 2161–2167.
[5] S.J. Singer, G.L. Nicolson, The fluid mosaic model of the structure of cell membranes, Science 175 (4023) (1972) 720–731.
[6] W.V. Humphreys, A. Walker, D. Charlesworth, Altered viscosity and yield stress in patients with abdominal malignancy: relationship to deep vein thrombosis, Br. J. Surg. 63 (7) (1976) 559–561.
[7] K.I. Karimov, B.U. Iriskulov, K.A. Askarov, Dynamic blood viscosity and liver microcirculation in alloxan diabetes associated with toxic hepatitis, Biulleten Eksp. Biol. Meditsiny 122 (7) (1996) 20–22.
[8] G. Deliconstantinos, V. Villiotou, J.C. Stavrides, Modulation of particulate nitric oxide synthase activity and peroxynitrite synthesis in cholesterol enriched endothelial cell membranes, Biochem. Pharmacol. 49 (11) (1995) 1589–1600.
[9] G.S. Zubenko, U. Kopp, T. Seto, L.L. Firestone, Platelet membrane fluidity individuals at risk for Alzheimer's disease: a comparison of results from fluorescence spectroscopy and electron spin resonance spectroscopy, Psychopharmacology 145 (2) (1999) 175–180.
[10] Z. Yang, Y. He, J.-H. Lee, N. Park, M. Suh, W.-S. Chae, J. Cao, X. Peng, H. Jung, C. Kang, J.S. Kim, A self-calibrating bipartite viscosity sensor for mitochondria, J. Am. Chem. Soc. 135 (24) (2013) 9181–9185.
[11] L. Wang, Y. Xiao, W. Tian, L. Deng, Activatable rotor for quantifying lysosomal viscosity in living cells, J. Am. Chem. Soc. 135 (8) (2013) 2903–2906.
[12] K. Luby-Phelps, Physical properties of cytoplasm, Curr. Opin. Cell Biol. 6 (1) (1994) 3–9.
[13] L. Ernster, G. Schatz, Mitochondria: a historical review, J. Cell Biol. 91 (3 Pt 2) (1981) 227s–255s.
[14] T. Finkel, Signal transduction by mitochondrial oxidants, J. Biol. Chem. 287 (7) (2012) 4434–4440.
[15] R. Del Bo, M. Moggio, M. Rango, S. Bonato, M.G. D'Angelo, S. Ghezzi, G. Airoldi, M.T. Bassi, M. Guglieri, L. Napoli, C. Lamperti, S. Corti, A. Federico, N. Bresolin, G. P. Comi, Mutated mitofusin 2 presents with intrafamilial variability and brain mitochondrial dysfunction, Neurology 71 (24) (2008) 1959–1966.
[16] S. Zuchner, P. De Jonghe, A. Jordanova, K.G. Claeys, V. Guergueltcheva, S. Cherninkova, S.R. Hamilton, G. Van Stavern, K.M. Krajewski, J. Stajich, I. Tournev, K. Verhoeven, C.T. Langerhorst, M. de Visser, F. Baas, T. Bird, V. Timmerman, M. Shy, J.M. Vance, Axonal neuropathy with optic atrophy is caused by mutations in mitofusin 2, Ann. Neurol. 59 (2) (2006) 276–281.
[17] T. Kalwarczyk, N. Ziebacz, A. Bielejewska, E. Zaboklicka, K. Koynov, J. Szymanski, A. Wilk, A. Patkowski, J. Gapinski, H.-J. Butt, R. Holyst, Comparative analysis of viscosity of complex liquids and cytoplasm of mammalian cells at the nanoscale, Nano Lett. 11 (5) (2011) 2157–2163.
[18] A.P. Minton, The influence of macromolecular crowding and macromolecular confinement on biochemical reactions in physiological media, J. Biol. Chem. 276 (14) (2001) 10577–10580.
[19] Y. Zhang, Y. Zhao, Y. Wu, B. Zhao, L. Wang, B. Song, Hemicyanine based naked-eye ratiometric fluorescent probe for monitoring lysosomal pH and its application, Spectrochim. Acta Mol. Biomol. Spectrosc. 227 (2020) 117767.
[20] F. Yu, X. Jing, W. Lin, Single-/Dual-Responsive pH fluorescent probes based on the hybridization of unconventional fluorescence and fluorophore for imaging lysosomal pH changes in HeLa cells, Anal. Chem. 91 (23) (2019) 15213–15219.
[21] Y. Dai, Y. Zheng, T. Xue, F. He, H. Ji, Z. Qi, A novel fluorescent probe for rapidly detection cysteine in cystinuria urine, living cancer/normal cells and BALB/c nude mice, Spectrochim. Acta Mol. Biomol. Spectrosc. 225 (2020) 117490.
[22] L. Zhao, X. He, Y. Huang, J. Li, Y. Li, S. Tao, Y. Sun, X. Wang, P. Ma, D. Song, A novel ESIPT-ICT-based near-infrared fluorescent probe with large Stokes-shift for

the highly sensitive, specific, and non-invasive in vivo detection of cysteine, Sensor. Actuator. B Chem. 296 (2019) 126571.
[23] L. Zhu, M. Fu, B. Yin, L. Wang, Y. Chen, Q. Zhu, A red-emitting fluorescent probe for mitochondria-target microviscosity in living cells and blood viscosity detection in hyperglycemia mice, Dyes Pigments 172 (2020) 107859.
[24] L. Yu, J.F. Zhang, M. Li, D. Jiang, Y. Zhou, P. Verwilst, J.S. Kim, Combining viscosity-restricted intramolecular motion and mitochondrial targeting leads to selective tumor visualization, Chem. Commun. 59 (2020) (2020) 6684–6687.
[25] L. Li, Y. Xu, Y. Chen, J. Zheng, J. Zhang, R. Li, H. Wan, J. Yin, Z. Yuan, H. Chen, A family of push-pull bio-probes for tracking lipid droplets in living cells with the detection of heterogeneity and polarity, Anal. Chim. Acta 1096 (2020) 166–173.
[26] Y. Dong, Z. Chen, M. Hou, L. Qi, C. Yan, X. Lu, R. Liu, Y. Xu, Mitochondria-targeted aggregation-induced emission active near infrared fluorescent probe for real-time imaging, Spectrochim. Acta Mol. Biomol. Spectrosc. 224 (2020) 117456.
[27] S. Li, P. Wang, W. Feng, Y. Xiang, K. Dou, Z. Liu, Simultaneous imaging of mitochondrial viscosity and hydrogen peroxide in Alzheimer's disease by a single near-infrared fluorescent probe with a large Stokes shift, Chem. Commun. 56 (7) (2020) 1050–1053.
[28] Y.J. Reo, Y.W. Jun, S. Sarkar, M. Dai, K.H. Ahn, Ratiometric imaging of gamma-glutamyl transpeptidase unperturbed by pH, polarity, and viscosity changes: a benzocoumarin-based two-photon fluorescent probe, Anal. Chem. 91 (21) (2019) 14101–14108.
[29] S. Sasaki, G.P.C. Drummen, G.-i. Konishi, Recent advances in twisted intramolecular charge transfer (TICT) fluorescence and related phenomena in materials chemistry, J. Mater. Chem. C 4 (14) (2016) 2731–2743.
[30] Y. Dou, Kenry, J. Liu, F. Zhang, C. Cai, Q. Zhu, 2-Styrylquinoline-based two-photon AIEgens for dual monitoring of pH and viscosity in living cells, J. Mater. Chem. B 7 (48) (2019) 7771–7775.
[31] X. Song, H. Bian, C. Wang, M. Hu, N. Li, Y. Xiao, Development and applications of a near-infrared dye-benzylguanine conjugate to specifically label SNAP-tagged proteins, Org. Biomol. Chem. 15 (38) (2017) 8091–8101.
[32] A.L. Stadler, J.O. Delos Santos, E.S. Stensrud, A. Dembska, G.L. Silva, S. Liu, N. I. Shank, E. Kunttas-Tatli, C.J. Sobers, P.M.E. Gramlich, T. Care, L.A. Peteanu, B. M. McCartney, B.A. Armitage, Fluorescent DNA nanotags featuring covalently attached intercalating dyes: synthesis, antibody conjugation, and intracellular imaging, Bioconjugate Chem. 22 (8) (2011) 1491–1502.
[33] G. Zhang, Y. Sun, X. He, W. Zhang, M. Tian, R. Feng, R. Zhang, X. Li, L. Guo, X. Yu, S. Zhang, Red-emitting mitochondrial probe with ultrahigh signal-to-noise ratio enables high-fidelity fluorescent images in two-photon microscopy, Anal. Chem. 87 (24) (2015) 12088–12095.
[34] A.S. Klymchenko, Solvatochromic and fluorogenic dyes as environment-sensitive probes: design and biological applications, Acc. Chem. Res. 50 (2) (2017) 366–375.
[35] M.A. Haidekker, T.T. Ling, M. Anglo, H.Y. Stevens, J.A. Frangos, E.A. Theodorakis, New fluorescent probes for the measurement of cell membrane viscosity, Chem. Biol. 8 (2) (2001) 123–131.
[36] M. Tang, Z. Huang, X. Luo, M. Liu, L. Wang, Z. Qi, S. Huang, J. Zhong, J.-X. Chen, L. Li, D. Wu, L. Chen, Ferritinophagy activation and sideroflexin1-dependent mitochondria iron overload is involved in apelin-13-induced cardiomyocytes hypertrophy, Free Radic. Biol. Med. 134 (2019) 445–457.
[37] Y. Liu, J. Zhou, L. Wang, X. Hu, X. Liu, M. Liu, Z. Cao, D. Shangguan, W. Tan, A cyanine dye to probe mitophagy: simultaneous detection of mitochondria and autolysosomes in live cells, J. Am. Chem. Soc. 138 (38) (2016) 12368–12374.
[38] C.W. Wang, D.J. Klionsky, The molecular mechanism of autophagy, Mol. Med. 9 (3–4) (2003) 65–76.